COMPARISON OF DIFFERENT CHAOTIC MAPS WITH APPLICATION TO IMAGE WATERMARKING

Athanasios Nikolaidis *Ioannis Pitas*

Department of Informatics
Aristotle University of Thessaloniki
Box 451, Thessaloniki 540 06, GREECE
e-mail: {nikola, pitas}@zeus.csd.auth.gr

ABSTRACT

The current paper presents a method for image watermarking based on chaotic sequences produced by different functions. The effect of embedding a chaotic watermark on an image is examined. Extensive experimental results for JPEG and filtering attacks on images watermarked by the different functions are presented together with a comparative study of them. The results show that efficient watermarking methods based on chaos can be designed under certain conditions.

1. INTRODUCTION

Image watermarking for copyright protection is a field that has drawn much attention in the latest years due to the wide spread of digital multimedia information through the internet. The main purpose is to protect copyrighted multimedia content from being attacked by malicious users during transmission, processing or storage.

Most of the proposed watermarking methods for still images are based on the construction of a pseudo-random sequence of real numbers that is afterwards somehow thresholded in order to provide a binary map which is the watermark to be embedded [1]-[3]. In this paper we present certain chaotic functions that can provide either controlled lowpass characteristics or good correlation properties. These are based on one-dimensional functions such as the Renyi map [4], as well as the N-way Bernoulli shift and the N-way tailed shift sequences which have already been used in telecommunication applications [5] because of the good correlation properties they possess. These watermarks prove to be robust to operations such as JPEG compression and lowpass filtering. A comparison of the performance of the different functions is presented, where detection ratios are defined by demanding certain false alarm ratio.

This work was funded by the LTR-ESPRIT European Project 31103-INSPECT.

2. GENERATION OF CHAOTIC FUNCTIONS

The first step in order to construct a chaos-based watermark is to define a recursive function that provides a sequence of real numbers. This is done by a mapping function $\mathbf{F} : U \rightarrow U, U \subset I\!R$. In the case of the Renyi map, the function is:

$$z(n+1) = \mathbf{F}(z(n), \lambda), \qquad z(n) \in U, \lambda \in I\!R \qquad (1)$$

where $n = 0, 1, 2, ...$ denotes the current iteration and λ is a parameter that controls the chaotic behavior of the system. This map for $\lambda = 1.2$ is depicted in Figure 1a.

The number of iterations is defined to be equal to the number of pixels in the image. The above mentioned functions produce sequences of theoretically infinite period.

For the Renyi map, by changing the value of the parameter λ, the set of real numbers is divided in two subsets U_{reg} and U_{ch}. If the initial value of the sequence belongs in U_{ch} the produced trajectory is chaotic. In our implementation the initial value is associated to the watermark key. We can define a threshold level z_{th} in a way that, after thresholding the sequence numbers, a bipolar sequence $s(n) \in \{-1, 1\}$ is produced with approximately equal number of -1s and 1s. Parameter λ controls the frequency characteristics of the chaotic sequence, i.e. the frequency of the transitions $-1 \rightarrow 1$ and $1 \rightarrow -1$. For $\lambda > 1$ and values close to 1, we get a chaotic watermark with low number of transitions and, thus, lowpass properties, whereas when $\lambda \simeq 2$ the transitions are very frequent, the lowpass properties degrade and the sequence is very similar to a pseudo-random one.

The shift functions mentioned in the previous section are a case of piecewise affine Markov maps. This means that they are piecewise linear over the interval $[0, 1]$ and the parameter n corresponds to the number of intervals where the function is linear. These functions produce chaotic sequences, irrespective of the initial value. However, there is no parameter that controls explicitly the lowpass characteristics for this class of functions. The form of the N-way

Bernoulli shift function is:

$$B(n+1) = \begin{cases} NB(n) & 0 \le B(n) < t_1 \\ N(B(n) - t_1) & t_1 \le B(n) < t_2 \\ \vdots & \vdots \\ N(B(n) - t_{n-1}) & t_{n-1} \le B(n) < t_n \end{cases} \quad (2)$$

whereas the form of the N-way tailed shift function is:

$$T(n+1) = \begin{cases} (N-1)T(n) + \frac{1}{N} & 0 \le T(n) < t_1 \\ (N-1)T(n) + \frac{2}{N} - 1 & t_1 \le T(n) < t_2 \\ \vdots & \vdots \\ (N-1)T(n) - \frac{N^2-3N+1}{N} & t_{n-2} \le T(n) < t_{n-1} \\ T(n) - \frac{N-1}{N} & t_{n-1} \le T(n) < t_n \end{cases} \quad (3)$$

The 3-way Bernoulli function and the 4-way tailed function are depicted in Figures 1b and 1c, respectively. These functions have the advantage that their cross correlation is very small for slight differences in the initial value of the sequence. This is essential for meeting the key uniqueness criterion. A thresholding step in order to create a binary map of equal number of 1s and -1s is followed as in the case of the Renyi map.

The sequence that is produced by using either function is one-dimensional. To embed it in a digital image, we need to scan across the sequence in such a way that the lowpass properties are preserved. This is useful especially for the case of the Renyi map approach. The classic raster scan is not proper for this task because the number of transitions is not any more under control in the vertical dimension. To avoid this we use Peano scan order which has better spatial properties than the raster scan. In addition, it is possible to use cellular smoothing to eliminate spontaneous transitions that emerged after the Peano scan [6]. Using this technique, the output watermark has local neighborhoods of 1s (or -1s) that are more compact.

In order to construct different watermarks we use a key K that produces the seed value for the generation of a chaotic trajectory. Keys of slightly different value provide sufficiently uncorrelated trajectories, because the set **K** of possible keys is quite large. This reduces the possibility of the watermark being tampered. It also ensures non-invertibility of the watermark. Thus, the corresponding key cannot be extracted from the two-dimensional watermark.

3. WATERMARK EMBEDDING

The smoothed two-dimensional watermark of size $2^n \times 2^n$ (due to the Peano scan) that is produced after the previous steps is scaled to the size of the image, if their sizes do not coincide. Before superimposing it on the original image, a visual masking stage could be introduced to avoid visual artifacts. However, it was not considered crucial to use visual masking in our experiments. The watermarked image $f_w(x,y)$ is defined as:

$$f_w(x,y) = f(x,y) + h(x,y) \cdot w(x,y) \quad (4)$$

where $w(x,y)$ is the bilevel sequence of 1s and -1s and $h(x,y)$ is the watermark power that is, in our case, constant:

$$h(x,y) = h \quad (5)$$

The watermark is to be casted in the spatial domain and, thus, the watermark power should be of an integer value.

4. WATERMARK DETECTION

When a prototype watermark is to be detected inside a watermarked and possibly manipulated image, the response of a hypothesis testing detector is computed:

$$R(\hat{f}_w, \hat{w}) = \frac{1}{N_{\mathbf{A}}} \sum_{(x,y)\in\mathbf{A}} \hat{f}_w(x,y) - \frac{1}{N_{\mathbf{B}}} \sum_{(x,y)\in\mathbf{B}} \hat{f}_w(x,y) \quad (6)$$

where the sets are $\mathbf{A} = \{(x,y)|\hat{w}(x,y) = 1\}$ and $\mathbf{B} = \{(x,y)|\hat{w}(x,y) = -1\}$. $N_{\mathbf{A}}$ and $N_{\mathbf{B}}$ are the number of pixels of the sets $\mathbf{A}$ and $\mathbf{B}$, respectively. In the case that the watermark is casted all over the image, without employing visual masking, the detector output is assumed to follow a normal distribution with mean value $\bar{R} = 2h$, where h is the watermark power. This means that if the watermark exists the detector output should be $R = 2h$, otherwise $R = 0$.

The response is computed over the entire image. The detector output (6) must be compared against a proper threshold R_{thr} that will inform us with a satisfying certainty about the presense or the absense of the watermark.

5. EXPERIMENTAL RESULTS

In order to test the robustness of the watermarking method to JPEG compression and lowpass filtering, we tested it on 5 color images (of size 960×960) depicting portable byzantine icons. The original watermark size was 1024×1024 and was constructed using Peano scan. The λ parameter was set to 1.2 for the Renyi function, and the n parameter was set to 3 for the Bernoulli shift and to 4 for the tailed shift. The method was tested for distortion of SNR 35dB and 30dB, corresponding to watermark power h of 2 and 3, respectively. 12 different compression ratios for JPEG were selected. Lowpass filtering was tested using moving average and median filters, both for windows of size 3×3 and 5×5. The detection threshold R_{thr} was chosen such that the false alarm ratio (FAR) was equal to 10^{-4} for every SNR level and for every chaotic function employed. The FAR was computed based on the empirical distributions provided by testing the method for 100 different watermarks. These watermarks were tested on both the image containing the

correct watermark and the image containing a false watermark. The experimental distributions of the detection responses were approximated by normal distributions.

Tables 1 and 2 show results for watermark detection after lowpass filtering for SNR values of 35dB and 30dB, respectively. We can observe that the 4-way tailed shift performs better than the 3-way Bernoulli shift and much better than the Renyi map. If we consider 98% as an acceptable detection ratio, only tailed shift gives good results for SNR = 35dB. However, all methods, except Renyi map for 5×5 moving average, perform well for SNR = 30dB. This implies that the tailed shift function resulted in the most lowpass watermark.

Figures 2a and 2b show results for 12 different compression ratios, for SNR values of 35dB and 30dB, respectively. The relative performance of the three functions is the same as in the case of lowpass filtering. For SNR = 35dB, tailed shift is robust for compression up to 1:40, Bernoulli shift up to 1:35 and Renyi map up to 1:30. Finally, all three functions give watermarks that are robust at least for compression up to 1:50, when SNR = 30dB.

We can see that though the Renyi map function contains a parameter that controls its lowpass properties, the shift functions give watermarks of finer details, for this size (1024×1024). The coarse watermark that is produced by the Renyi map results in different watermarks having a rather high correlation and, thus, giving distributions of larger variance. As a result, in order to meet the desired FAR (10^{-4}) a rather big threshold is required and, thus, more correct watermarks are discarded. For smaller SNR values, that is, for stronger watermarks, the variance is decreased and, correspondingly, the threshold is also decreased, resulting in larger detection ratios for the same FAR.

6. CONCLUSIONS

In the present paper we tested several chaotic functions for embedding and detecting watermarks in color images. The watermark, when possible, was chosen such as to possess certain lowpass characteristics or correlation properties. A hypothesis testing detector was employed in order to decide about the presense of a potential watermark. Experimental results display the robustness of the different functions to JPEG compression and lowpass filtering. The most robust watermarks proved to be the ones produced by the N-way tailed shift function, whereas the Renyi map watermarks are the less resistant to attacks.

7. REFERENCES

[1] N. Nikolaidis and I. Pitas, "Copyright Protection of Images using Robust Digital Signatures", in *Proc. of the IEEE Int. Conf. on Acoustics, Speech and Signal Processing, ICASSP '96*, May 1996, Atlanta, Georgia, vol. 4, pp. 2168-2171.

[2] I.J. Cox, J. Killian, T. Leighton and T. Shamoon, " Secure Spread Spectrum Watermarking for Multimedia", in *IEEE Trans. on Image Processing*, **6**(12), pp. 1673-1687.

[3] A. Piva, M. Barni, F. Bartolini and V. Capellini, "DCT-based watermark recovering without resorting to the uncorrupted original image", in *Proc. IEEE Int. Conf. on Image Processing (ICIP'97)*, October 1997, Santa Barbara, California, vol. 1, pp. 520-523, 1997.

[4] A. Lasota and M.C. Mackey, "Chaos, Fractals, and Noise", Springer-Verlag, 2nd edition, 1994.

[5] R. Rovatti, G. Setti and G. Mazzini, "Chaotic Complex Spreading Sequences for Asynchronous DS-CDMA - Part II: Some Theoretical Performance Bounds", in *IEEE Trans. on Circuits and Systems I: Fundamental Theory and Applications*, **45**(4), pp. 496-506.

[6] G. Voyatzis and I. Pitas, "Chaotic Watermarks for Embedding in the Spatial Digital Image Domain", in *Proc. of ICIP '98*, October 1998, Chicago, Illinois, vol. 2, pp. 432-436.

Filter	Bernoulli	Renyi	Tailed
Moving Average 3×3	100	100	100
Moving Average 5×5	82.8	38.8	98.6
Median 3×3	100	100	100
Median 5×5	99.8	91.8	100

Table 1: Detection ratios for lowpass attacks on images of SNR=35dB.

Filter	Bernoulli	Renyi	Tailed
Moving Average 3×3	100	100	100
Moving Average 5×5	100	94.4	100
Median 3×3	100	100	100
Median 5×5	100	100	100

Table 2: Detection ratios for lowpass attacks on images of SNR=30dB.

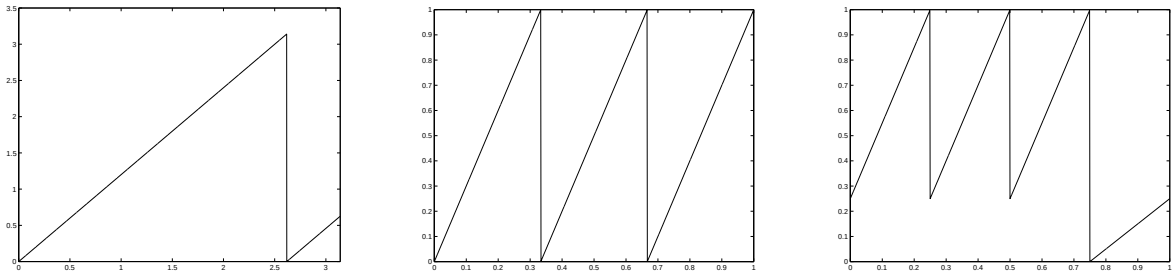

(a) (b) (c)

Figure 1: (a) Renyi map for $\lambda = 1.2$. (b) Bernoulli map for $N = 3$. (c) Tailed map for $N = 4$.

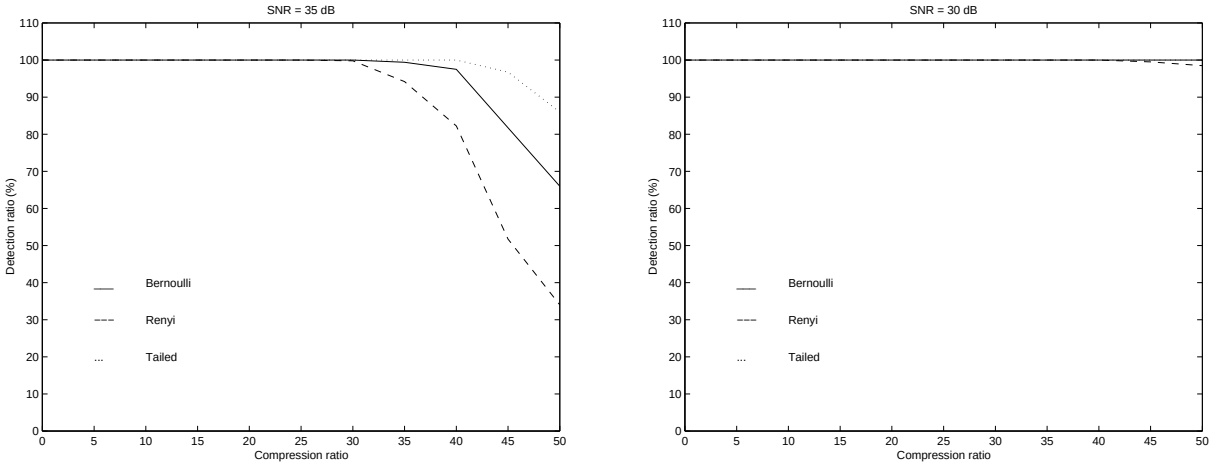

(a) (b)

Figure 2: (a) Detection ratio for JPEG compression on images of SNR=35dB. (b) Detection ratio for JPEG compression on images of SNR=30dB.